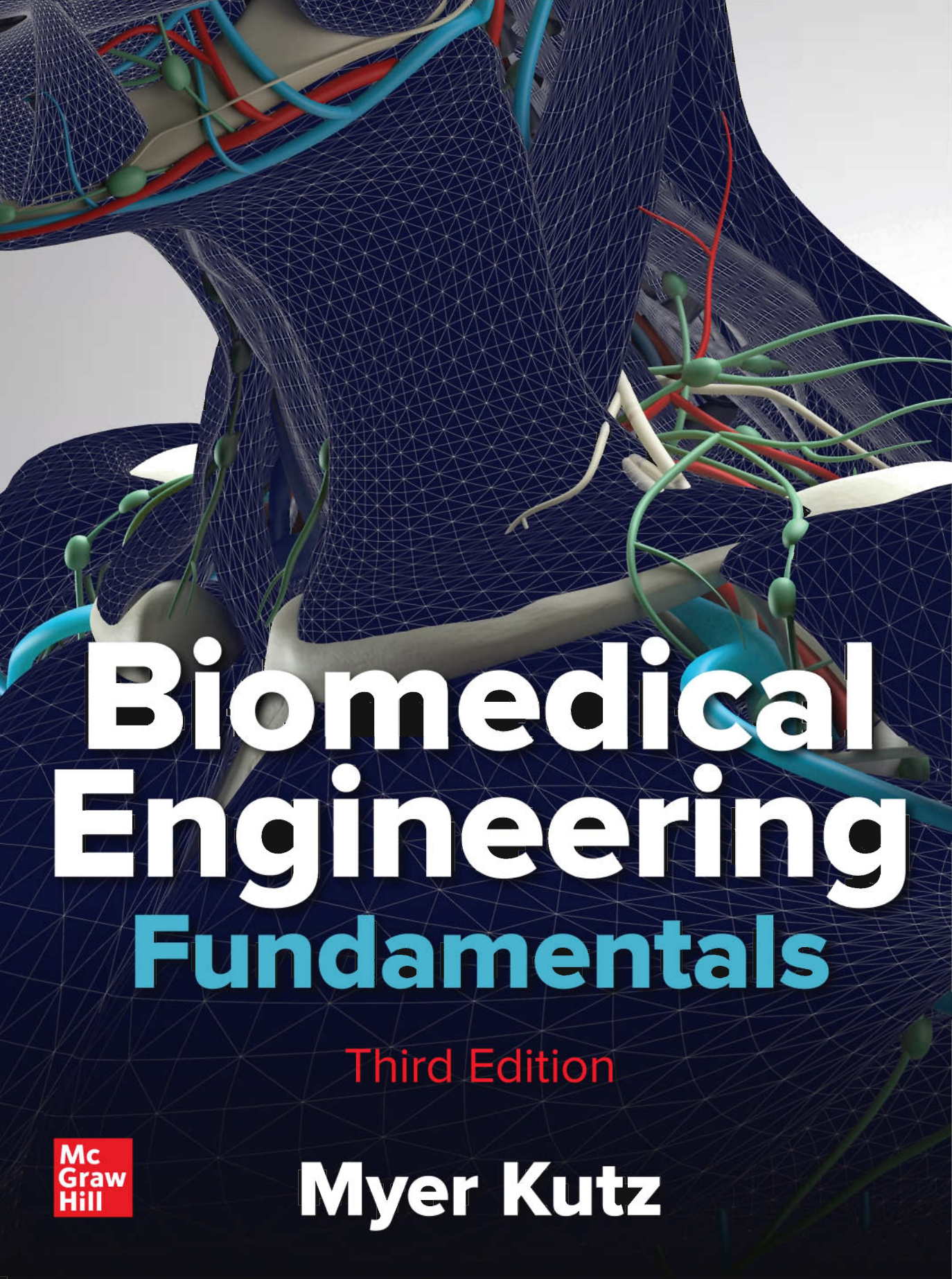

Biomedical Engineering Fundamentals

Third Edition

Mc Graw Hill

Myer Kutz

BIOMEDICAL ENGINEERING FUNDAMENTALS

BIOMEDICAL ENGINEERING FUNDAMENTALS

Myer Kutz Editor

Third Edition

New York Chicago San Francisco Athens London
Madrid Mexico City Milan New Delhi
Singapore Sydney Toronto

Library of Congress Control Number: 2020952464

Biomedical Engineering Fundamentals, Third Edition

1 2 3 4 5 6 7 8 9 CCD 26 25 24 23 22 21

ISBN 978-1-260-13626-5
MHID 1-260-13626-4

This book is printed on acid-free paper.

Sponsoring Editor
Robin Najar

Editing Supervisor
Stephen M. Smith

Production Supervisor
Pamela A. Pelton

Acquisitions Coordinator
Elizabeth M. Houde

Project Manager
Jyoti Shaw, MPS Limited

Copy Editor
Mohammad Taiyab Khan, MPS Limited

Proofreader
Nikhil Roshan

Indexer
Edwin Durbin

Art Director, Cover
Jeff Weeks

Composition
MPS Limited

For Arlene, forever

ABOUT THE EDITOR

MYER KUTZ is founder and president of Myer Kutz Associates, Inc., a publishing and information services consulting firm.

CONTENTS

CONTRIBUTORS

Crystal Anderson-Cunanan *Boston Scientific Corporation, Marlborough, Massachusetts* (Chap. 18)

Ronald E. Barr *University of Texas, Austin, Texas* (Chap. 9)

Christopher Batich *University of Florida, Gainesville, Florida* (Chap. 15)

Ravi V. Bellamkonda *Georgia Institute of Technology/Emory University, Atlanta, Georgia* (Chap. 21)

Anthony J. Brammer *University of Connecticut Health, Farmington, Connecticut* (Chap. 13)

Thomas S. Buchanan *University of Delaware, Newark, Delaware* (Chaps. 8, 14)

Hsiang-Han Chen *University of Minnesota, Minneapolis, Minnesota* (Chap. 3)

Vladimir Cherkassky *University of Minnesota, Minneapolis, Minnesota* (Chap. 3)

Shmuel Einav *Tel Aviv University, Tel Aviv, Israel* (Chap. 5)

David Elad *Tel Aviv University, Tel Aviv, Israel* (Chaps. 5, 7)

Michele J. Grimm *Michigan State University, East Lansing, Michigan* (Chap. 20)

Paul Grimshaw *University of Adelaide, Adelaide, Australia* (Chap. 11)

James B. Grotberg *University of Michigan, Ann Arbor, Michigan* (Chap. 6)

Pinchas Halpern *Tel Aviv Medical Center, Tel Aviv, Israel, and Sackler School of Medicine, Tel Aviv University, Tel Aviv, Israel* (Chap. 7)

Michael N. Helmus *Medical Devices, Drug Delivery, and Nanotechnology, Worcester, Massachusetts* (Chap. 18)

William Hersh *Oregon Health & Science University, Portland, Oregon* (Chap. 2)

Arif Iftekhar *University of Minnesota, Minneapolis, Minnesota* (Chap. 16)

Dentcho Ivanov *Microelectronics Fabrication Center, New Jersey Institute of Technology, Newark, New Jersey* (Chap. 25)

Teena James *Department of Biomedical Engineering and Microelectronics Research Center, New Jersey Institute of Technology, Newark, New Jersey* (Chap. 25)

Chris Jones *Independent Researcher, Adelaide, Australia* (Chap. 11)

Tony M. Keaveny *University of California, San Francisco, California, and University of California, Berkeley, California* (Chap. 10)

David H. Kohn *University of Michigan, Ann Arbor, Michigan* (Chap. 17)

Patrick Leamy *LifeLink Foundation, Tampa, Florida* (Chap. 15)

Hyunjung Lee *Georgia Institute of Technology, Atlanta, Georgia* (Chap. 21)

Merilyn Lock *University of South Australia, Adelaide, Australia* (Chap. 11)

Eric J. Madsen *University of Michigan, Ann Arbor, Michigan* (Chap. 17)

Kurt T. Manal *University of Delaware, Newark, Delaware* (Chap. 8)

Manu Sebastian Mannoor *Department of Biomedical Engineering and Microelectronics Research Center, New Jersey Institute of Technology, Newark, New Jersey* (Chap. 25)

Nancy J. Meilander *National Institute of Standards and Technology, Gaithersburg, Maryland* (Chap. 21)

Elise F. Morgan *University of California, Berkeley, California* (Chap. 10)

Jit Muthuswamy *Arizona State University, Tempe, Arizona* (Chaps. 23, 26)

Roger J. Narayan *University of North Carolina and North Carolina State University, Raleigh, North Carolina* (Chap. 24)

Michael D. Nowak *University of Hartford, West Hartford, Connecticut* (Chap. 12)

Govind Pandey *King George Medical University, Lucknow, India* (Chap. 24)

Prem C. Pandey *Banaras Hindu University, Varanasi, India* (Chap. 24)

Marcus G. Pandy *University of Melbourne, Melbourne, Australia* (Chap. 9)

Donald R. Peterson *Northern Illinois University, DeKalb, Illinois* (Chap. 13)

Bonnie Pierson *University of North Carolina and North Carolina State University, Raleigh, North Carolina* (Chap. 24)

Shrirang V. Ranade *Genentech Inc., a member of the Roche Group, South San Francisco, California* (Chap. 18)

Anat Ratnovsky *Afeka College of Engineering, Tel Aviv, Israel* (Chap. 7)

Narender P. Reddy *University of Akron, Akron, Ohio* (Chap. 1)

Qi Shao *University of Delaware, Newark, Delaware* (Chap. 14)

Bruce C. Towe *Arizona State University, Tempe, Arizona* (Chap. 22)

Bradley Jay Willenberg *University of Central Florida, Orlando, Florida* (Chap. 15)

Oscar C. Yeh *University of California, Berkeley, California* (Chap. 10)

Roya Zandparsa *Tufts University School of Dental Medicine, Boston, Massachusetts* (Chap. 19)

Liang Zhu *University of Maryland, Baltimore County, Baltimore, Maryland* (Chap. 4)

PREFACE

The purpose of this handbook is to provide engineers, physicians, and other medical professionals with fundamental information that will help them use engineering sensibilities and methodologies to invent, design, properly operate, and evaluate medical instruments, devices, and machines. This third edition is an expanded and updated version of Vol. 1, *Fundamentals*, of the *Biomedical Engineering and Design Handbook,* Second Edition, published in the summer of 2009, and follows the same outline. Again, there are four major parts: Biomedical Systems Analysis, which now has three chapters instead of one; Biomechanics of the Human Body, with 11 chapters in both editions; Biomaterials, with seven chapters in both editions; and Bioelectronics, with five chapters in both editions.

Of the 26 chapters in the third edition—two chapters more than in the second edition—four chapters are entirely new and nine have been updated. Two second edition chapters have been dropped: Biodynamics: A Lagrangian Approach and Biomedical Signal Processing. I should point out that the first volume of the second edition constituted a substantial revision of the corresponding parts of the first edition. So the overall revision from first to third editions has been extensive, in keeping with the growth of knowledge in the biomedical engineering discipline.

The four new chapters in this edition cover the following important topics, which add value for readers: Biomedical Informatics (Chap. 2, contributed by William Hersh), which deals with the efficient storage, acquisition, and use of information in healthcare; Machine Learning for Biomedical Engineering (Chap. 3, contributed by Vladimir Cherkassky and Hsiang-Han Chen), which involves methodological issues and assumptions important for applying machine learning to biomedical data so that limitations of predictive data-analytic models can be understood properly, available data can be modeled mathematically, and the right questions can be asked of the data; Biomechanics of the Foot and Knee (Chap. 11, contributed by Paul Grimshaw, Chris Jones, and Merilyn Lock), fundamental knowledge which underlies, for example, treatment of injury to the anterior cruciate ligament; and Neural Interfaces (Chap. 26, contributed by Jit Muthuswamy), which can be implanted so that electrical activity from single neurons in the brain and peripheral nervous system can be recorded.

As noted above, nine chapters from the second edition have been updated for this edition. Comments regarding those updates are presented in the following paragraphs.

Liang Zhu, contributor of Chap. 4, Heat Transfer Applications in Biological Systems, writes: "There are quite a lot of updates due to my teaching of bioheat transfer and my research in the past 10 years. In addition to the major updates, including some figures, many new references after 2007 were added to the manuscript." Among the sections updated are those dealing with the Pennes bioheat equation, bioheat transfer modeling, temperature, thermal properties and blood flow measurements, hyperthermia, and thermal damage assessment.

Marcus G. Pandy, co-contributor with Ronald E. Barr, of Chap. 9, Biomechanics of the Musculoskelatal System, writes: "I have removed the text that appeared in the very last section of the previous version and replaced this with a description of running biomechanics, which I believe the reader will find interesting plus it follows nicely from the description of walking biomechanics appearing immediately above. I also have included two new figures."

In Chap. 12, Finite-Element Analysis, contributor Michael D. Nowak has added text on coronary artery disease, vascular assist devices, and aortic valve replacement, plus two complex figures.

Donald R. Peterson, co-contributor with Anthony J. Brammer, of Chap. 13, Vibration, Mechanical Shock, and Impact, writes: "The chapter has significant updates as some of the

second edition version is obsolete now." Among the sections with major updates are Biodynamic Models in the section on Models and Human Surrogates; Occurrence of Health Effects and Injury in the section on Countermeasures; Protection against Hand-Transmitted Vibration in the section on Countermeasures.

In Chap. 15, Polymeric Biomaterials, the contributors, led by Christopher Batich, added an extensive new section on biocompatibility and tissue engineering by Bradley Jay Willenberg, as well as a major new section on sterilization by Patrick Leamy. Part of the section on tissue scaffolds has been rewritten.

David H. Kohn, co-contributor of Chap. 17, Bioceramics, writes: "The main changes to the chapter included an expansion of the inorganic/organic hybrid section, especially discussion of peptide conjugation to calcium phosphates and nanotechnology."

Michael N. Helmus, co-contributor of Chap. 18, Cardiovascular Biomaterials, wrote to me with a lengthy list of changes, including updates to tables that were in the second edition; addition of new tables, together with discussion; a new section, Special Risks Associated with the Use of Materials of Animal Origin; plus five new discussions on other topics.

Michele J. Grimm, contributor of Chap. 20, Orthopedic Biomaterials, writes: "Sections on mechanobiology were added to the discussions of bone, cartilage, and ligament/tendon. References were updated where key new information was available (e.g., tantalum, zirconia, calcium sulfate injectables, wear particles, metal-on-metal hip implants, and others). A section on biodegradable metal was added."

Chapter 24, Biosensors (lead contributor, Roger J. Narayan), was updated with several changes to the text and the addition of two figures.

Although the majority of this handbook's contributors work in the United States, there is a noteworthy international component. Contributors of two chapters, Biomechanics of the Musculoskelatal System, which was updated, and Biomechanics of the Foot and Knee, which is new, are located in Australia. Two chapters, carried over unchanged from the second edition, were written by contributors located in Israel. A co-contributor of the chapter on Vibration, Mechanical Shock, and Impact is based part-time in Canada, and contributors of updates to the chapter on Biosensors are located in India. Most contributors work in academia, with a smattering of them in industry and government. I am immensely grateful to all of the contributors—those who contributed new and updated chapters, as well as those whose chapters from the second edition have been carried over unchanged into this one. I know how difficult it is to find the time to do any kind of writing, particularly a scholarly chapter on a technical subject, in these days when professionals in academia and industry are so hard-pressed. Thank you all.

Thanks also to my wonderful wife, Arlene, whose love is the thing I cherish most in all the world.

Myer Kutz
Delmar, New York

P · A · R · T · 1

BIOMEDICAL SYSTEMS ANALYSIS

CHAPTER 1
MODELING OF BIOMEDICAL SYSTEMS

Narender P. Reddy
University of Akron, Akron, Ohio

Models are conceptual constructions which allow formulation and testing of hypotheses. A mathematical model attempts to duplicate the quantitative behavior of the system. Mathematical models are used in today's scientific and technological world due to the ease with which they can be used to analyze real systems. The most prominent value of a model is its ability to predict as yet unknown properties of the system. The major advantage of a mathematical or computer model is that the model parameters can be easily altered and the system performance can be simulated. Mathematical models allow the study of subsystems in isolation from the parent system. Model studies are often inexpensive and less time consuming than corresponding experimental studies. A model can also be used as a powerful educational tool since it permits idealization of processes. Models of physiological systems often aid in the specification of design criteria for the design of procedures aimed at alleviating pathological conditions. Mathematical models are useful in the design of medical devices. Mathematical model simulations are first conducted in the evaluation of the medical devices before conducting expensive animal testing and clinical trials. Models are often useful in the prescription of patient protocols for the use of medical devices. Pharmacokinetic models have been extensively used in the design of drugs and drug therapies.

There are two types of modeling approaches: the black box approach and the building block approach. In the black box approach, a mathematical model is formulated based on the input-output characteristic of the system without consideration of the internal functioning of the system. Neural network models and autoregressive models are some examples of the black box approach. In the building block approach, models are derived by applying the fundamental laws (governing physical laws) and constitutive relations to the subsystems. These laws together with physical constraints are used to integrate the models of subsystems into an overall mathematical model of the system. The building block approach is used when the processes of the system are understood. However, if the system processes are unknown or too complex, then the black box approach is used. With the building block approach, models can be derived at the microscopic or at the macroscopic levels. Microscopic models are spatially distributed and macroscopic models are spatially lumped and are rather

global. The microscopic modeling often leads to partial differential equations, whereas the macroscopic or global modeling leads to a set of ordinary differential equations. For example, the microscopic approach can be used to derive the velocity profile for blood flow in an artery; the global or macroscopic approach is needed to study the overall behavior of the circulatory system including the flow through arteries, capillaries, and the heart. Models can also be classified into continuous time models and models lumped in time domain. While the continuous time modeling leads to a set of differential equations, the models lumped in time are based on the analysis of discrete events in time and may lead to difference equations or sometimes into difference-differential equations. Random walk models and queuing theory models are some examples of discrete time models. Nerve firing in the central nervous system can be modeled using such discrete time event theories. Models can be classified into deterministic and stochastic models. For example, in deterministic modeling, we could describe the rate of change of volume of an arterial compartment to be equal to rate of flow in minus the rate of flow out of the compartment. However, in the stochastic approach, we look at the probability of increase in the volume of the compartment in an interval to be dependent on the probability of transition of a volume of fluid from the previous compartment and the probability of transition of a volume of fluid from the compartment to the next compartment. While the deterministic approach gives the means or average values, the stochastic approach yields means, variances, and covariances. The stochastic approach may be useful in describing the cellular dynamics, cell proliferations, etc. However, in this chapter, we will consider only the deterministic modeling at the macroscopic level.

The real world is complex, nonlinear, nonhomogeneous, often discontinuous, anisotropic, multilayered, multidimensional, etc. The system of interest is isolated from the rest of the world using a boundary. The system is then conceptually reduced to that of a mathematical model using a set of simplifying assumptions. Therefore, the model results have significant limitations and are valid only in the regimes where the assumptions are valid.

1.1 COMPARTMENTAL MODELS

Compartment models are lumped models. The concept of a compartmental model assumes that the system can be divided into a number of homogeneous well-mixed components called compartments. Various characteristics of the system are determined by the movement of material from one compartment to the other. Compartment models have been used to describe blood flow distribution to various organs, population dynamics, cellular dynamics, distribution of chemical species (hormones and metabolites) in various organs, temperature distribution, etc.

Physiological systems (e.g., cardiovascular system) are regulated by humoral mediators and can be artificially controlled using drugs. For instance, the blood pressure depends on vascular resistance. The vascular resistance in turn can be controlled by vasodilators. The principle of mass balance can be used to construct simple compartment models of drug distribution. Figure 1.1 shows a general multicompartmental (24-compartment) model of drug distribution in the human body. The rate of increase of mass of a drug in a compartment is equal to the rate of mass flowing into the compartment minus the rate of mass leaving the compartment, minus the rate of consumption of the drug due to chemical reaction in the compartment. In the model shown in Fig. 1.1, the lungs are represented by three compartments: Compartment 3 represents the blood vessels (capillaries, etc.) of the lung, the interstitial fluids of the lung are represented by compartment 4, and the intracellular components of the lung are represented by compartment 5. Each other organ (e.g., kidneys) is represented by two compartments consisting of the blood vessels (intravascular) and the tissue (extravascular consisting of interstitial and intracellular components together). Let us consider the model equations for a few compartments.

For compartment 3 (lung capillaries),

$$V_3 dC_3/dt = Q_2 C_2 - Q_3 C_3 - K_{3\text{-}4} A_{3\text{-}4} (C_3 - C_4) \tag{1.1}$$

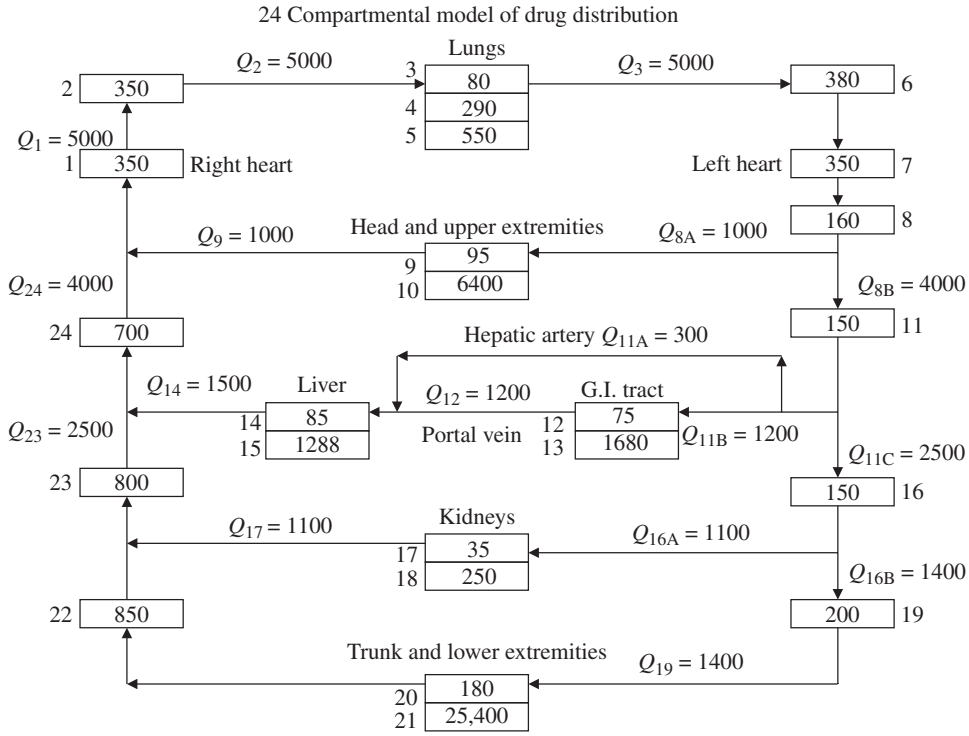

FIGURE 1.1 A generalized multicompartment (24) model of the human body to analyze drug distribution in the body. The numbers in the compartments represent volumes in milliliters. The numbers on the lines are flow rates in mL/min.

Q_2C_2 is the rate of mass flowing into compartment 3 from compartment 2, and Q_3C_3 is the rate of mass flowing out of compartment 3 into compartment 6. In addition, there is the interface mass transfer (diffusion) from capillaries into the interstitial spaces. This is represented by the last term. $K_{3\text{-}4}$ is the diffusional permeability of lung capillary. The diffusional permeability depends on capillary pore size, the number of pores per unit area, the diffusion coefficient for the drug molecule, the ratio of the diameter of the drug molecule, and the pore diameter. This permeability is different from the hydraulic permeability. $A_{3\text{-}4}$ is the lung capillary (interface) surface area. Mass is equal to volume times concentration. The change in volume occurs over a longer duration when compared to the changes in concentration. Consequently, volumes are assumed to be constant.

For the interstitial compartment,

$$V_4 dC_4/dt = K_{3\text{-}4}A_{3\text{-}4}(C_3 - C_4) - K_{4\text{-}5}A_{4\text{-}5}(C_4 - C_5) \tag{1.2}$$

For the intracellular compartment,

$$V_5 dC_5/dt = K_{4\text{-}5}A_{4\text{-}5}(C_4 - C_5) - M_R \tag{1.3}$$

where M_R is the rate of metabolic consumption of the drug. This could be a constant at high concentrations and a function of concentration at low concentrations. Recently, Kim et al. (2007) have developed a whole body glucose homeostasis during exercise and studied the effect of hormonal control.

Simple one compartmental models can be used for the prescription of treatment protocols for dialysis using an artificial kidney device. While the blood urea nitrogen (BUN) concentration in the

normal individual is usually 15 mg% (mg% = milligrams of the substance per 100 mL of blood), the BUN in uremic patients could reach 50 mg%. The purpose of the dialysis is to bring the BUN level closer to the normal. In the artificial kidney, blood flows on one side of the dialyzer membrane and dialysate fluid flows on the other side. Mass transfer across the dialyzer membrane occurs by diffusion due to concentration difference across the membrane. Dialysate fluid consists of a makeup solution consisting of saline, ions, and the essential nutrients so as to maintain zero concentration difference for these essential materials across the membrane. However, during the dialysis, some hormones also diffuse out of the dialyzer membrane along with the urea molecule. Too rapid dialysis often leads to depression in the individual due to the rapid loss of hormones. On the other hand, too slow dialysis may lead to unreasonable time required at the hospital. Simple modeling can be used to calculate the treatment protocols of mass coming into the body from the dialyzer, plus the metabolic production rate. When the patient is *not* on dialysis, the concentration of urea would increase linearly if the metabolic production rate is constant or will increase exponentially if the metabolic production rate is a linear function of the concentration (first-order reaction). When the patient is *on* dialysis, the concentration would decrease exponentially. This way, the treatment protocol can be prescribed after simulating different *on* and *off* times (e.g., turn on the dialyzer for 4 hours every 3 days) to bring the BUN under control. In the chapter on artificial kidney devices, a simple one compartmental model is used to compute the patient protocol.

Compartmental models are often used in the analysis of thermal interactions. Simon and Reddy (1994) formulated a mathematical model of the infant-incubator dynamics. Neonates who are born preterm often do not have the maturity for thermal regulation and do not have enough metabolic heat production. Moreover, these infants have a large surface area to volume ratio. Since these preterm babies cannot regulate heat, they are often kept in an incubator until they reach thermal maturity. The incubator is usually a forced convection heating system with hot air flowing over the infant. Incubators are usually designed to provide a choice of air control or the skin control. In air control, the temperature probe is placed in the incubator air space and the incubator air temperature is controlled. In the skin control operation, the temperature sensor is placed on the skin and infant's skin temperature is controlled. Simon et al. (1994) used a five-compartmental model (Fig. 1.2) to compare the adequacy of air control and skin control on the core temperature of the infant. They considered the infant's core, infant's skin, incubator air, mattress, and the incubator wall to be four separate well-mixed compartments.

The rate of change of energy in each compartment is equal to the net heat transfer via conduction, convection, radiation, evaporation, and the sensible heat loss. There is a convective heat loss from the infant's core to the skin via the blood flow to the skin. There is also conductive heat transfer from the core to the skin. The infant is breathing incubator air, drawing in dry cold air at the incubator air temperature and exhaling humidified hot air at body temperature. There is heat transfer associated with heating the air from incubator air temperature to the infant's body (core) temperature. In addition, there is a convective heat transfer from the incubator air to the skin. This heat transfer is forced convection when the hot air is blowing into the incubator space and free convection when the heater manifolds are closed. Moreover, there is an evaporative heat loss from the skin to the incubator air. This is enhanced in premature infants as their skin may not be mature. Also, there is a conductive heat transfer from the back surface of the skin to the mattress. Also, exposed skin may radiate to the incubator wall. The incubator air is receiving hot air (convective heat transfer) from the hot air blower when the blower is in the *on* position. There is convective heat transfer from the incubator air to the incubator wall and to the mattress. In addition, there is metabolic heat production in the core. The energy balance for each compartment can be expressed as

$$mCp(dT/dt) = \Sigma Q_{\text{in}} - \Sigma Q_{\text{out}} + G \tag{1.4}$$

where m is the mass of the compartment, T is the temperature, t is the time, Q is the heat transfer rate, and G is the metabolic heat production rate. G is nonzero for the core and zero for all other compartments. G is low in low-birth-weight and significantly premature babies. Simon et al. (1994) investigated infant-incubator dynamics in normal, low birth weight, and different degrees of prematurity under skin and air control. Recently, Reddy et al. (2008) used the lumped compartmental

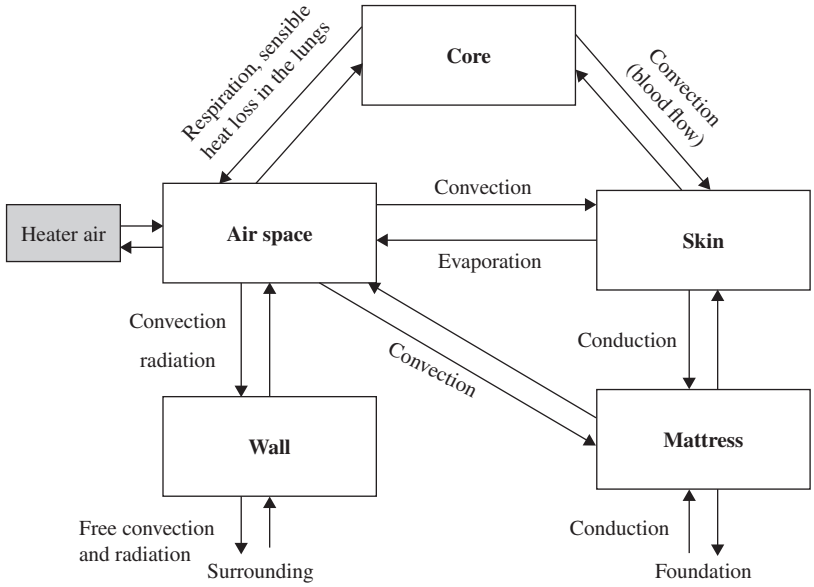

FIGURE 1.2 A lumped parameter model of the infant-incubator dynamics used by Simon et al. (1994) to simulate the effect of various control modes in a convectively heated infant incubator. Infant's core and skin are modeled as two separate compartments. The incubator air space, the incubator wall, and the mattress are treated as three compartments. Heat interactions occur between the core (infant's lungs) and the incubator air space through breathing. Skin-core heat interactions are predominantly due to blood flow to the skin. Heat transfer between the infant's skin and the incubator air is due to conduction and convection. Heat transfer from the skin to the mattress is via conduction, and heat transfer to the wall is via radiation from skin and convection from the air.

model of Simon et al. (1994) to evaluate the efficacy of air control, skin, control, and fuzzy logic control which incorporates both skin and air temperatures.

Compartmental models have been used to model particle dynamics. The growing number of cases of lung diseases, related to the accumulation of inhaled nonsoluble particles, has become a major problem in the urban population. Sturm (2007) has developed a simple multicompartment model for the clearance of nonsoluble particles from the tracheobronchial system (Fig. 1.3). While most of the particles are rapidly transported toward the pharynx by the beating celia, the particles caught in between celia in the highly viscous gel layer (compartment 1) may enter the low viscous sol layer (compartment 2) via diffusion. From the sol layer, they could enter the epithelium (compartment 5) and eventually enter the regional lymph node (compartment 6) or enter the blood circulation. Alternatively, they could be captured by the macrophages (compartment 4) in any of these layers and could reach the regional lymph node or the blood circulation (compartment 6) or the gastrointestinal tract (GIT; compartment 3). Macrophages could release phagocytosed particles into any of these layers. In addition, the particles could defuse among all three layers (gel, sol, and epithelium) in both directions. Sturum (2007) has derived model equations based on the diffusion of particles and other modes of transport.

1.2 ELECTRICAL ANALOG MODELS OF CIRCULATION

Electric analog models are a class of lumped models and are often used to simulate flow through the network of blood vessels. These models are useful in assessing the overall performance of a system or a subsystem. Integration of the fluid momentum equation (longitudinal direction, in cylindrical

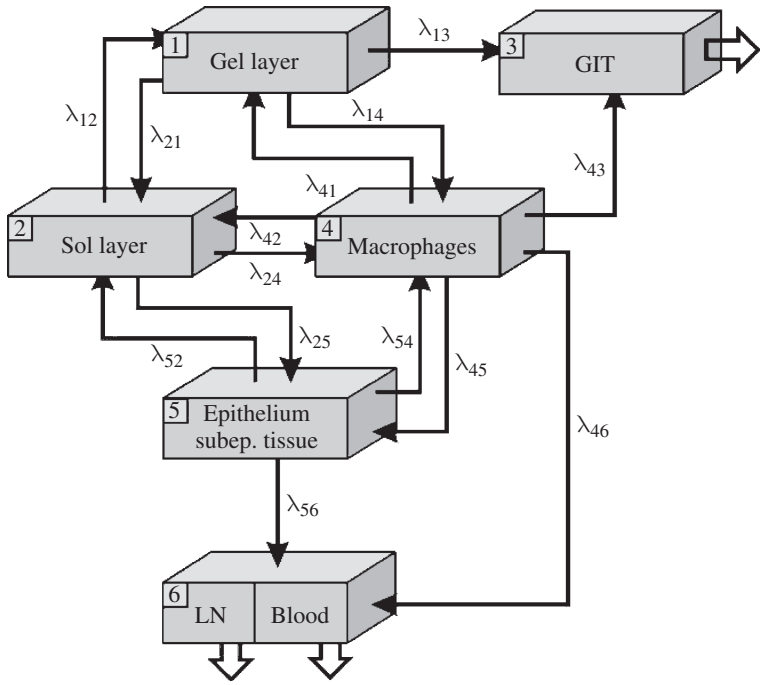

FIGURE 1.3 A multicompartmental model for the clearance of inhaled insoluble particles from the lung. [*Reproduced with permission from Sturm (2007).*]

coordinates) across the cross section results in the following expression (Reddy, 1986; Reddy and Kesavan, 1989):

$$\rho dQ/dt = \pi a^2 \, \Delta P/\ell 2a\tau_w \tag{1.5}$$

where ρ is the fluid density, Q is the flow rate, a is the wall radius, P is the pressure, ℓ is the length, and τ_w is the fluid shear stress at the wall. If we assume that the wall shear stress can be expressed using quasisteady analysis, then the wall shear stress can be estimated by $\tau_w = 4\mu Q/a^3$. Upon substituting for the wall stress and rearranging, the results are

$$[\rho\ell/(\pi a^2)]dQ/dt = \Delta P - [8\mu\ell/(\pi a^4)]Q \tag{1.6}$$

The above equation can be rewritten as

$$LdQ/dt = \Delta P - RQ \tag{1.7}$$

where $L = \rho\ell/(\pi a^2)$ and $R = 8\mu\ell/(\pi a^4)$.

It can be easily observed that flow rate Q is analogous to electrical current i, and ΔP is analogous to the electrical potential drop (voltage) ΔE. In the above equation, L is the inductance (inertance) and R is the resistance to flow. Therefore, Eq. (1.5) can be rewritten as

$$Ldi/dt = \Delta \overline{E} - Ri \tag{1.8}$$

Fluid continuity equation, when integrated across the cross section, can be expressed as

$$dV/dt = \Delta Q = Q_{\text{in}} - Q_{\text{out}} \tag{1.9}$$

where V is the volume. However, volume is a function of pressure. Momentum balance for the vessel wall can be expressed as

$$P = P_{ext} + (h/a_0)\sigma \tag{1.10}$$

where P_{ext} is the external pressure on the outside of the vessel wall, h is the wall thickness, and σ is the hoop stress in the wall. The hoop stress is a function of wall radius a and modulus of elasticity E of the wall, and can be expressed as

$$\sigma = (E/2)[(a/a_0)^2 - 1] \tag{1.11}$$

where a_0 is the unstretched radius. Since the length of the segment does not change, the above equation can be expressed as

$$\sigma = (E/2)[(V/V_0) - 1] \tag{1.12}$$

where V is the volume of the vessel segment and V_0 is the unstretched volume. Equations (1.10), (1.11), and (1.12) can be combined as

$$dV/dt = CdP/dt \tag{1.13}$$

where

$$C = (2V_0\, a_0/hE) \tag{1.14}$$

C is often referred to as the compliance or capacitance.

Substituting Eq. (1.13) in Eq. (1.9) results in

$$CdP/dt = Q_{in} - Q_{out} \tag{1.15}$$

Equation (1.15) can be expressed in terms of an electrical equivalent as follows:

$$\overline{E} = (1/C)\int i dt \tag{1.16}$$

Equations (1.7) and (1.16) can be used to simulate either a segment of a blood vessel or the entire blood vessel itself. In small blood vessels, the inductance L is very low when compared to the resistance term R, and therefore, the inductance term can be neglected in small arteries, arterioles, and capillaries. Since there is no oscillation of pressure in the capillaries, the inductance term can be neglected in vessels downstream of the capillary including venules, veins, vena cava, etc. (Chu and Reddy, 1992).

An electrical analog model of the circulation in the leg is illustrated in Fig. 1.4. Let us consider the flow from the femoral artery into the small leg arteries. There is no inductance in small leg arteries, and there is only the resistance. Since the small arteries are distensible, they have capacitance (compliance). The muscular pressure (P_{MP}) acts as the external pressure on the majority of small leg arteries. Consequently, P_{MP} is used as the reference pressure across the capacitor. The arterioles do not have inductance, but have a variable resistance which is controlled by neurogenic and metabolic factors. In this model, the precapillary sphincters and the capillaries are lumped together. Since the capillaries are rather rigid, they do not have any capacitance (compliance), but the combined resistance of the sphincters and capillaries is variable subject to metabolic control. For instance, precapillary sphincters dilate in the presence of lactic acid and other end products of metabolism. Venules have resistance and a variable capacitance. This capacitance is subject to neurogenic control since the diameter of the venule is under neurogenic control. From the venules, the flow goes into leg small veins which have a resistance and a variable capacitance subject to neurogenic control. In addition, the venules have valves which only permit unidirectional flow. These valves can be modeled as diodes. Again, the reference pressure for the capacitor is the muscle pressure P_{MP}. It is well known that the blood flow in the legs is aided by the muscle pump which is essentially the external pressure oscillations on the blood vessel wall due to periodic skeletal muscle contractions during walking, etc. The muscle pump is absent in bedridden patients. Extremity pumps are used on such patients to enhance blood flow to the legs. These extremity pumps provide a periodic a graded sequential external compression of the leg. The electrical analog model shown in Fig. 1.4 can be easily modified to simulate the effect of these extremity pumps.

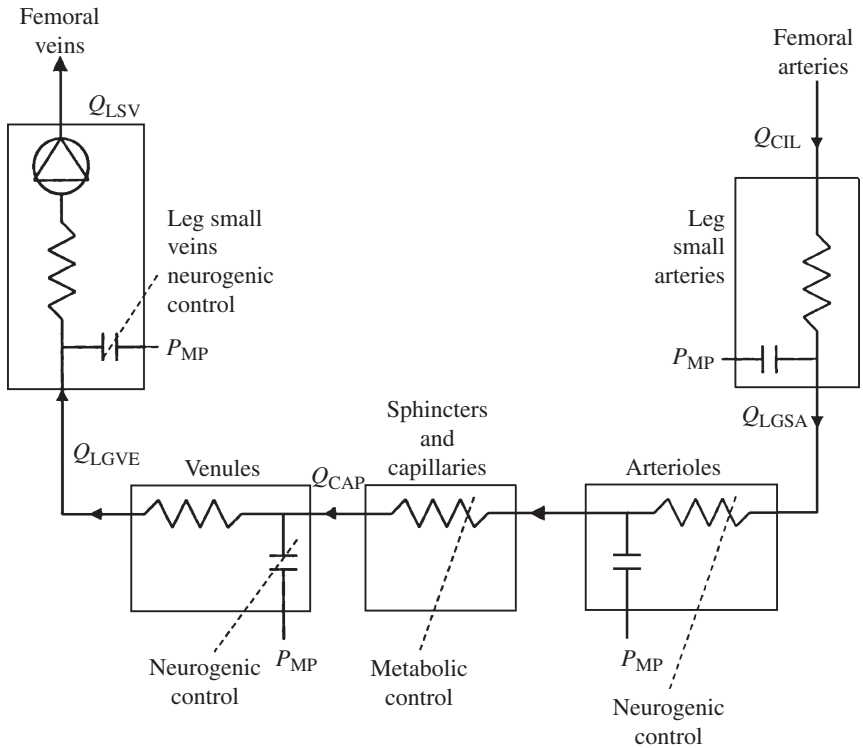

FIGURE 1.4 Electrical analog model of the circulation of the leg P_{MP} is the muscle pump which exerts a periodic external pressure on the blood vessels, Q is the flow rate, Q_{LGSA} is the flow through the leg small arteries, Q_{CAP} is the flow rate through the capillary, and Q_{LGVE} is the flow through the leg small veins. The elasticity is simulated with capacitance. The nonlinear capacitance of the leg small veins and the nonlinear resistance of arterioles and venules are under neurogenic control. The resistance of precapillary sphincters and capillaries is subject to metabolic control. The valves in the veins are simulated using diodes which permit only the unidirectional flow.

An electric analog model of pulmonary circulation is shown in Fig. 1.5. The flow is considered from node to node where the pressure is defined. The model equations for flow from compartment 1 (right ventricle) to the pulmonary arteries can be expressed by

$$L(dQ_1/dt) = P_1 - P_2 - R_1Q_1 \tag{1.17}$$

The pressure in compartment 2 can be expressed as

$$P_2 - P_{i\text{th}} = (1/C_1)\int(Q_1 - Q_2)dt \tag{1.18}$$

where $P_{i\text{th}}$ is the intrathoracic pressure, which is pressure acting on the outside of the pulmonary vessels. Similarly,

$$P_2 - P_3 = R_2Q_2 \tag{1.19}$$

$$P_3 - P_{i\text{th}} = (1/C_2)\int(Q_2 - Q_3)dt \tag{1.20}$$

$$P_3 - P_5 = R_3Q_3 \tag{1.21}$$

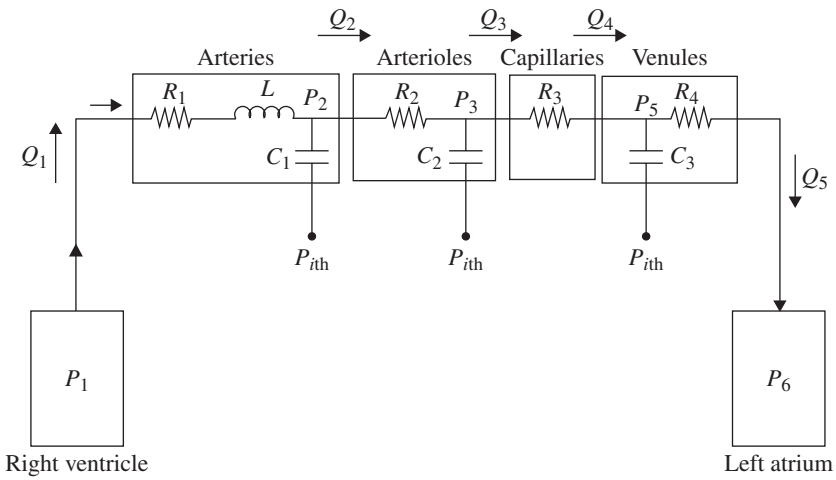

FIGURE 1.5 A model of pulmonary circulation. P_{ith} is the intrathoracic pressure which is the external pressure on the pulmonary blood vessels.

$$P_5 - P_{i\text{th}} = (1/C_3)\int(Q_4 - Q_5)dt \tag{1.22}$$

$$Q_3 = Q_4 \tag{1.23}$$

$$P_5 - P_6 = R_4 Q_5 \tag{1.24}$$

The capacitance is due to distensibility of the vessel. The capillaries are stiffer and less distensible, and therefore have minimal capacitance.

Electrical analog models have been used in the study of cardiovascular, pulmonary, intestinal, and urinary system dynamics. Recently, Barnea and Gillon (2001) have used an electrical analog model to simulate flow through the urethra. Their model consisted of a simple L, R, C circuit with a variable capacitor. The time varying capacitor simulated the time-dependent relaxation of the urethra. They used two types of resistance: a constant resistance to simulate Poiseouille-type viscous pressure drop and a flow-dependent resistance to simulate Bernoulli-type pressure loss. With real-time pressure-flow data sets, Barnea and Gillon (2001) have used the model to estimate urethral resistance and changes in urethral compliance during voiding, and have suggested that the urethral elastance (inverse of compliance) estimated by the model provides a new diagnostic tool. Ventricular and atrial pumping can be modeled using similar techniques. The actual pump (pressure source) can be modeled as a variable capacitor. Figure 1.6 shows a model of the left heart with a multisegment representation of the ventricle (Rideout, 1991). Kerckhoffs et al. (2007) have coupled an electrical analog model of systemic circulation with a finite element model of cardiac ventricular mechanics.

1.3 MECHANICAL MODELS

Mechanical models consisting of combinations of springs and dashpots are very popular in numerous disciplines. Spring dashpot models have been used to model the mechanical behavior of viscoelastic materials and can be used to represent the one dimensional behavior of tissue and other biological materials. In a linear spring, the force is proportional to the change in length or the strain.

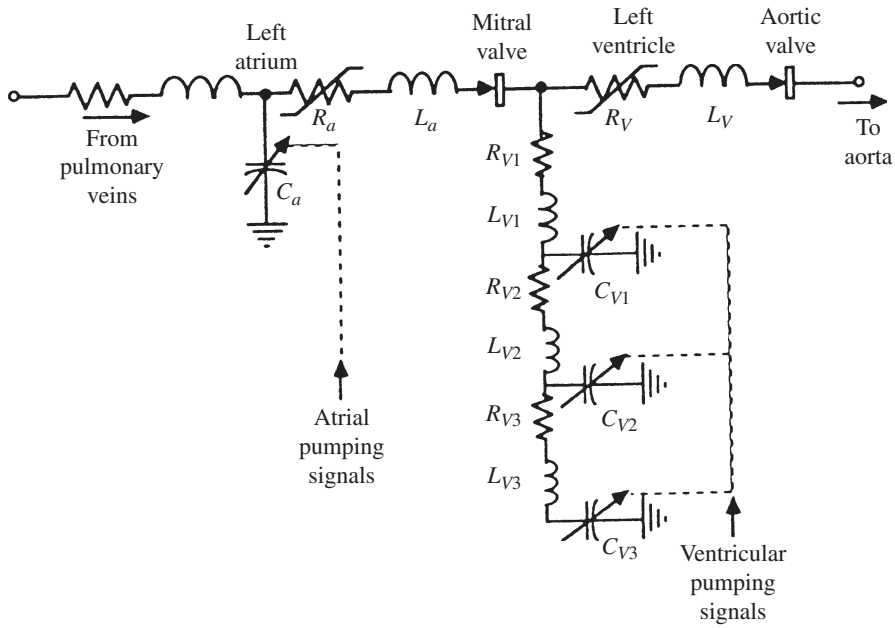

FIGURE 1.6 Electrical analog model to simulate atrial and ventricular pumping. Variable capacitances simulate the muscle contractions, and the filling and emptying through the ventricle can be simulated by a series of inductance and resistance elements. [*Adapted from Rideout (1991).*]

On the other hand, the force in a dashpot is proportional to the rate of change in strain. Consider a mass supported by a spring and a dashpot in parallel. Let a force F be acting on the mass. Force in a dashpot is $b(dX/dt)$ since the force in a fluid depends on strain rate. Here, b is a constant. The force in the spring is given by kX, where k is the spring constant.

Application of Newton's law results in

$$m(d^2X/dt^2) + b(dX/dt) + kX = F \tag{1.25}$$

where X is the elongation or change in length with respect to the steady-state value, b is the constant of the dashpot, and k is the spring constant.

It should be pointed out that the above mechanical equation is similar to the following electrical equation:

$$L(di/dt) + Ri + (1/C)\int i dt = E \tag{1.26}$$

where L is the inductance, R is the resistance, i is the current, and E is the voltage. This equation can be expressed in terms of the charge q instead of the current as

$$L(d^2q/dt^2) + R(dq/dt) + (1/C)q = E \tag{1.27}$$

Equations (1.25), (1.26), and (1.27) are similar. Therefore, mass is analogous to the inductance, the dashpot is analogous to the resistor, and the spring is analogous to the capacitor. The spring and the capacitor are storage units, whereas the dashpot and the resistor are the dissipaters of energy. The charge is analogous to the deformation or elongation, the current is similar to the velocity, and force is analogous to the voltage. Therefore, any electrical system can be modeled using mechanical analogs and any mechanical system can be modeled using electrical analogs.

Lumped mechanical models have been used to analyze the impact dynamics. Generally, muscle is represented by a combination of a spring and a dashpot, whereas a ligament is modeled using a spring.

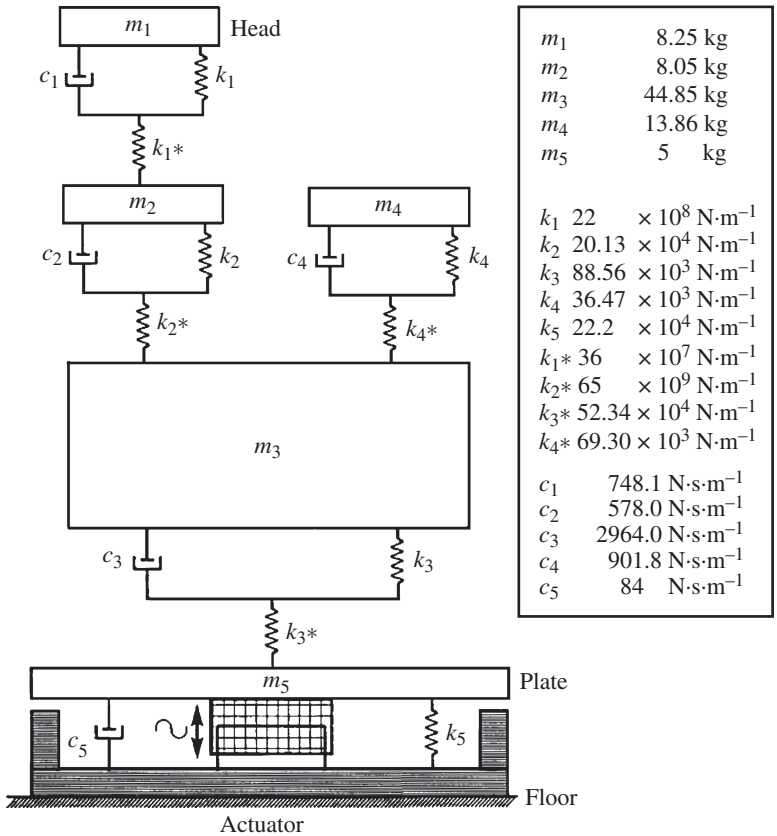

m_1	8.25 kg
m_2	8.05 kg
m_3	44.85 kg
m_4	13.86 kg
m_5	5 kg
k_1	22 $\times 10^8$ N·m^{-1}
k_2	20.13 $\times 10^4$ N·m^{-1}
k_3	88.56 $\times 10^3$ N·m^{-1}
k_4	36.47 $\times 10^3$ N·m^{-1}
k_5	22.2 $\times 10^4$ N·m^{-1}
k_1*	36 $\times 10^7$ N·m^{-1}
k_2*	65 $\times 10^9$ N·m^{-1}
k_3*	52.34 $\times 10^4$ N·m^{-1}
k_4*	69.30 $\times 10^3$ N·m^{-1}
c_1	748.1 N·s·m^{-1}
c_2	578.0 N·s·m^{-1}
c_3	2964.0 N·s·m^{-1}
c_4	901.8 N·s·m^{-1}
c_5	84 N·s·m^{-1}

FIGURE 1.7 A lumped mechanical analog model for the analysis of vibration in relaxed standing human. [*Reproduced with permission from Fritton et al. (1997).*]

Human body vibrations can be analyzed using similar lumped models. Fritton et al. (1997) developed a lumped parameter model (Fig. 1.7) to analyze head vibration and vibration transmissibility in a standing individual. The model results are in good agreement with the experimental results. Such models are useful in the design of automobile seat cushion, motorcycle helmet design, etc.

1.4 MODELS WITH MEMORY AND MODELS WITH TIME DELAY

Time delay and memory processes occur in several biomedical disciplines. An example of such an application occurs in modeling of the immune system (Reddy and Krouskop, 1978). In cellular immune response, lymphocytes are sensitized to a foreign material and have memory. The immune response is significantly enhanced if the similar material is reintroduced after certain lag time. Another example could be the application to stress-induced bone remodeling. Modeling of the nervous system would involve time delays and memory. Similar hereditary functions are used to describe the material responses of viscoelastic materials. The effect of environmental pollutants can be modeled using such hereditary functions. Stress-induced bone remodeling involves time lags between the actual application of stress and actual new bone formation, and also involves

stress/strain histories. To illustrate the modeling of the effects of memory and time delay, let us consider a model to predict the number of engineers in the United States. Then we will consider a model of cell-mediated immunity which has similar delays and memory functions.

1.4.1 A Model to Predict the Number of Engineers in the United States

An easy-to-understand example of a deterministic model with time delay and memory is a model to predict the number of biomedical engineers in the United States at any given time. Let us restrict our analysis to a single discipline such as biomedical engineering. Let E be the number of engineers (biomedical) at any given time. The time rate of change of the number of engineers at any given time in the United States can be expressed as

$$dE/dt = G + I - R - L - M \tag{1.28}$$

where G represents the number of graduates entering the profession (graduating from an engineering program) per unit time, I represents the number of engineers immigrating into the United States per unit time, R represents the number of engineers retiring per unit time, L represents the number of engineers leaving the profession per unit time (e.g., leaving the profession to become doctors, lawyers, managers, etc.), and M represents the number of engineers dying (before retirement) per unit time.

In Eq. (1.28), we have lumped the entire United States into a single region (a well-stirred compartment) with homogeneous distribution. In addition, we have not made any discrimination with regard to age, sex, or professional level. We have considered the entire pool as a well-stirred homogeneous compartment. In reality, there is a continuous distribution of ages. Even with this global analysis with a lumped model, we could consider the age distribution with a series of compartments with each compartment representing engineers within a particular age group. Moreover, we have assumed that all engineering graduates enter the workforce. A percentage of them go to graduate school and enter the workforce at a later time.

The number of graduates entering the profession is a function of the number of students entering the engineering school 4 years before:

$$G(t) = k_1 S(t - 4) \tag{1.29}$$

where $S(t)$ is the number of students entering the engineering school per unit time. The number of students entering the engineering school depends on the demand for the engineering profession over a period of years, that is, on the demand history.

The number of engineers immigrating into the United States per unit time depends on two factors: demand history in the United States for engineers and the number of visas that can be issued per unit time. Assuming that immigration visa policy is also dependent on demand history, we can assume that I is dependent on demand history. Here we have assumed that immigrants from all foreign countries are lumped into a single compartment. In reality, each country should be placed in a separate compartment and intercompartmental diffusion should be studied.

The number of engineers retiring per unit time is proportional to the number of engineers in the profession at the time:

$$R(t) = k_2 E(t) \tag{1.30}$$

The number of engineers leaving the profession depends on various factors: the demand for the engineering profession at that time and demand for various other professions at that time as well as on several personal factors. For the purpose of this analysis, let us assume that the number of engineers leaving the profession in a time interval is proportional to the number of individuals in the profession at that time:

$$L(t) = k_3 E(t) \tag{1.31}$$

The number of engineers dying (before retirement) per unit time is proportional to the number of engineers at that time:

$$M(t) = k_4 E(t) \tag{1.32}$$

The demand for engineers at any given time is proportional to the number of jobs available at that time ($J(t)$) and is inversely proportional to the number of engineers available at that time:

$$D(t) = kJ(t)/E(t) \tag{1.33}$$

The number of jobs available depends on various factors such as government spending for R&D projects, economic growth, sales of medical products, number of hospitals, etc. Let us assume in this case (biomedical engineering) that the number of jobs is directly proportional to the sales of medical products (p), directly proportional to government spending for health care R&D (e), and directly proportional to the number of new medical product company startups (i):

$$J(t) = (k_6 e + k_7 c + k_8 i + k_9 + kp) \tag{1.34}$$

Although we assumed that the number of jobs at the present time is dependent on $e(t)$, $c(t)$, $h(t)$, $i(t)$, and $p(t)$, in reality the number of jobs at present may depend on previous values of these parameters, or on the history of these parameters.

Let us now analyze the demand history. This history depends on the memory function. Let us assume that the effect of demand existing at a time decays exponentially (exponentially decaying memory). The net effect of demands from time = 0 to t can be expressed as

$$H_1(t) = {}_{\tau=0} I^{\tau=t}\{D(\tau)\exp[-k_{10}(t-\tau)]\}d\tau \tag{1.35}$$

The number of students entering the engineering school per unit time is

$$S(t) = k_{11} H_1(t) \tag{1.36}$$

Immigration rate can similarly be expressed as

$$I(t) = k_{12} H_2(t) \tag{1.37}$$

where

$$H_2(t) = {}_{\tau=0} I^{\tau=t}\{D(\tau)\exp[-k_{13}(t-\tau)]\}d\tau \tag{1.38}$$

H_1 and H_2 are called hereditary functions. Instead of an exponential decay of memory, we could have a sinusoidal or some other functional form of memory decay, depending on the physical situation.

$$dE/dt = k_1 k_{10} H_1(t-4) + k_{11} H_2(t) - (k_2 + k_3 + k_4)E(t) \tag{1.39}$$

In this analysis, making various assumptions, we have formulated a lumped parameter deterministic model to predict the number of engineers (biomedical) present in the United States at any given time. If we want to know the geographical distribution, we can take two approaches. We can divide the entire United States into a number of compartments (e.g., northeast, east, west, etc.) and study the intercompartmental diffusion. Alternatively, we can make E a continuous variable in space and time I (x, y, t) and account for spatial diffusion.

1.4.2 Modeling the Cell-Mediated Immunity in Homograft Rejection

In cell-mediated immunity, lymphocytes in the tissue become sensitized to the target (graft) cells and travel to the regional lymph nodes where they initiate an immunological response by increasing the production of immunocompetent lymphocytes. The newly produced lymphocytes are then transported

into the blood stream via the thoracic duct. Lymphocytes recirculate from the blood stream through the tissue and return to the blood stream via the lymphatic system. When foreign cells are introduced into the tissue, blood lymphocytes migrate into the tissue at an increased rate and bring about the destruction of the target cells. Lymphocytes have memory and they exhibit an increased secondary response, e.g., if after the rejection of the first graft, a second graft is introduced into the host, the second graft is rejected much faster. A similar situation occurs in delayed hypersensitivity, which is another cell-mediated reaction. In this analysis, let us assume that blood and tissue are well-stirred compartments and that the newly produced lymphocytes are introduced into the blood compartment (Reddy and Krouskop, 1978).

For sensitization to occur, a lymphocyte has to come in contact with a target cell. The number of lymphocytes becoming sensitized at any given time ($L_s(t)$) is a function of the number of lymphocytes in the tissue ($L_T(t)$) and the number of target (foreign) cells ($g(t)$)

$$L_s(t) = C_1 L_T(t) g(t) \tag{1.40}$$

Certain lymphocytes, upon encountering target cells, are transformed into memory cells. The memory cell formation depends upon the number of lymphocytes in the tissue and the number of target cells. The number of memory cells formed at any time (t) may thus be expressed as

$$L_{\text{ms}}(t) = C_1 L_T(t) g(t) \tag{1.41}$$

Sensitized lymphocytes stimulate the production of immunocompetent lymphocytes and the effect of each sensitized cell lasts for a given period of time. For the purpose of the present analysis, it is assumed that the effect of each sensitized lymphocyte decays exponentially over a period of time. The production rate of blood lymphocytes at any time (t) due to the primary response $(dL_B/dt)_{\text{prim}}$ would then be equal to the sum of the residual effect of all the lymphocytes sensitized between time 0 and time $t - \Phi_1$, where Φ_1 is the time lag between sensitization and production of the lymphocytes.

The number of lymphocytes produced due to primary response between time t and time $(t - \Phi_1)$ would be

$$L_B(t) - L_B(t - \Delta t) = C_3\{\underbrace{L_S(t - \Phi_1)\Delta t}_{\substack{\text{Due to lymphocytes}\\ \text{sensitized at } t - \Phi_1}} + \underbrace{L_S(t - \Phi_1 - \Delta t)\Delta t}_{\substack{\text{Due to lymphocytes}\\ \text{sensitized at } t - \Phi_1 - \Delta t}} + \underbrace{L_S(t - \Phi_1 - 2\Delta t)e^{-K1\Delta t}\Delta t}_{\substack{\text{Due to lymphocytes}\\ \text{sensitized at } t - 2\Phi_{1-} - \Delta t}}$$

$$+ \underbrace{L_S(t - \Phi_1 - r\Delta t)e^{-K1\, r\Delta t}\Delta t}_{\substack{\text{Due to lymphocytes}\\ \text{sensitized at } t - \Phi_{1-} = r\Delta t}} + \cdots\} \tag{1.42}$$

$$= C_3 3 L_S(t - \Phi_1 - r\Delta t)e^{-K1\, r\Delta t}\Delta t \tag{1.43}$$

Dividing by Δt and taking the limits as $\Delta t \;\Pi\; 0$, the left-hand side becomes a derivative and the right-hand side can be represented as an integral in terms of the hereditary function

$$(dL_B(t)/dt)_{\text{primary}} = C_3 \int_0^{t - \Phi 1} L_S(\tau) e^{-K1(t - \Phi_1 - \tau)} d\tau \tag{1.44}$$

Substituting for L_S in terms of L_T,

$$(dL_B(t)/dt)_{\text{primary}} = k_2 \int_0^{t - \Phi 1} L_T(\tau) e^{-K1(t - \Phi_1 - \tau)} d\tau \tag{1.45}$$

For the secondary response to appear, a memory cell must encounter a target cell, and therefore the secondary response depends upon the number of memory cells and the number of target cells. Similar to (Eq. 1.45), Reddy and Krouskop (1978) expressed the secondary response in terms of a hereditary function

$$(dL_B(t)/dt)_{\text{secondary}} = k_3 \int_0^{t - \Phi 2} L_T(\tau) g(\tau) e^{-K4(t - \Phi_2 - \tau)} g(t - \Phi_3) d\tau \tag{1.46}$$